Vortex dynamics in a coarsening two-dimensional *XY* model

Hai Qian and Gene F. Mazenko
James Franck Institute and Department of Physics, University of Chicago, Chicago, Illinois 60637, USA
(Received 16 April 2003; published 20 August 2003)

The vortex velocity distribution function for a two-dimensional coarsening nonconserved O(2) time-dependent Ginzburg-Landau model is determined numerically and compared to theoretical predictions. In agreement with these predictions the distribution function scales with the average vortex speed which is inversely proportional to t^x, where t is the time after the quench and x is near 1/2. We find the entire curve, including a large speed algebraic tail, in good agreement with the theory.

DOI: 10.1103/PhysRevE.68.021109 PACS number(s): 65.60.+a, 66.70.+f, 63.20.Ry, 66.35.+a

I. INTRODUCTION

It is important to understand the role of defects in phase ordering [1] problems. We investigate here the growth kinetics of the nonconserved O(2) symmetric time-dependent Ginzburg-Landau (TDGL) model in two dimensions after a quench from a disordered high temperature state to zero temperature. The dominant structures in the ordering kinetics of this system are vortices with charges ± 1. Vortices with higher order charges are unstable. Various aspects of the defect structure have been explored in some detail before [2,3]. We focus here on a numerical determination of the velocity distribution of the vortices as a function of time t after the quench. Theory predicts [4] that the distribution function scales with the average vortex speed which is inversely proportional to a length scale $L(t)$, which grows with time t after the quenches. One also finds a large speed algebraic tail in good agreement with predictions of an exponent of -3. In terms of the velocity distribution this corresponds to an exponent of -4. The number of vortices is also counted and its evolution in time is found to be consistent with previous work [5].

The disordering agents in the phase ordering of the $n=d=2$ nonconserved TDGL model ($2dXY$ model) are well known, where d is the spatial dimension and n is the number of the components of the order parameter. One has unit-1 charged vortices and, at nonzero temperature, spin waves. If we focus on quenches to zero temperature, we have only the vortices to consider. Thus a typical vortex configuration is shown in Fig. 1. As the time evolves one has vortex antivortex annihilation until finally there are no surviving vortices and the system is fully ordered (we only consider the zero-temperature case with no thermal fluctuations, where the system does eventually order). For general $n=d$, Rutenberg and Bray [6] have shown that the growth law for such systems is given by $L(t)\approx t^{1/2}$. The exception is for $n=d=2$ where their method is mute. The growth law for this case was treated by Pargellis *et al.* [7], and checked numerically by Yurke *et al.* [5]. There is a logarithmic correction to the scaling law: $L(t)\approx[t/\log(t)]^{1/2}$.

There has also been theoretical work on the dynamics of these vortices. Mazenko [4] showed that if the order parameter can be assumed to be a Gaussian field [8] when constrained to be near a vortex core, then the vortex velocity probability distribution, for $n=d$ [4,9], has the simple form

$$P(\vec{v})d^n v=\frac{\Gamma(1+n/2)}{(\pi s^2)^{n/2}}\frac{1}{(1+v^2/s^2)^{(n+2)/2}}d^n v, \qquad (1)$$

where the scaling speed s varies as L^{-1} for long times. If we only care about the magnitude of the velocity and integrate out the directions, then in the case of $n=d=2$ we have the speed probability distribution

$$P(v)\,dv=\frac{2}{s^2}\frac{v}{(1+v^2/s^2)^2}dv,$$

or equivalently

$$P(\tilde{v})\,d\tilde{v}=\frac{2a\,\tilde{v}}{(1+a\tilde{v}^2)^2}d\tilde{v}, \qquad (2)$$

with $a=(\pi/2)^2$ and $\tilde{v}=v/\overline{v}$, where the average speed $\overline{v}=\pi s/2$. So, after being scaled with the average speed, the

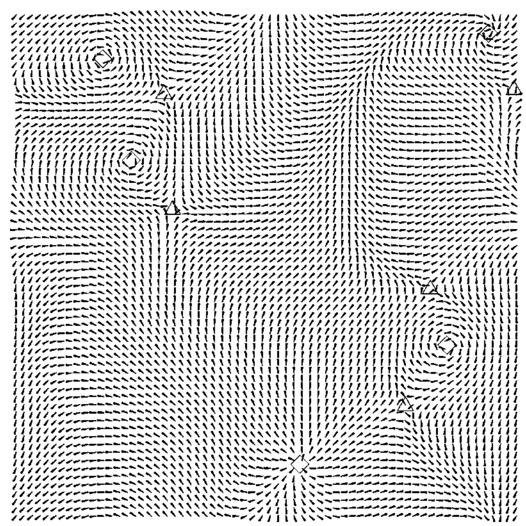

FIG. 1. A typical vortex configuration in a 256×256 system with lattice spacing $\Delta r=\pi/4$. The arrow on each each site represents the order parameter at that point. Not all the lattice sites are shown. The squares and triangles are in the core regions of $+1$ and -1 vortices, respectively, where the magnitude of the order parameter is near zero. The vortex core regions are picked out by using the method described in the text.

vortex speeds have the same probability distribution at different times. A key feature of the predictions for $P(v)$ is that there is a large velocity algebraic tail $\sim v^{-3}$. This tail was also found using scaling arguments by Bray [10]. In this paper we check these predictions numerically for the case $n=d=2$. We find that velocity probability distribution function does obey scaling of the form predicted by Eq. (2). But the average speed falls off as $t^{-1/2}$ without the logarithmic correction, and there is a large speed tail consistent with an exponent of -3.

We have also monitored the vortex density n_v as a function of time and find, in agreement with previous work [5],

$$n_v \propto L_v^{-2}(t), \tag{3}$$

where $L_v(t) \propto [t/\ln(t)]^{1/2}$. The vortex number density should be proportional to the system's energy above its ground energy E_0 $(=-\epsilon^2/4)$ per unit area, where ϵ is the control parameter of the system [see Eq. (4) below]. Our simulation verifies this result.

II. SYSTEM DESCRIPTION

The system we study is described by the Langevin equation

$$\frac{\partial \psi_i}{\partial t} = \epsilon \psi_i + \nabla^2 \psi_i - (\vec{\psi})^2 \psi_i, \tag{4}$$

where $i=1,2$ are the indices for the two components of the order parameter $\vec{\psi}$. The noise term is zero because the system is quenched to zero temperature. By choosing proper units for the time and space and rescaling the order parameter, ϵ can take on any positive value. The equation is put on a square lattice with periodic boundary conditions and driven by the finite difference scheme, i.e., replacing $\partial_t \psi_i(\mathbf{r},t)$ by $[\psi_i^{m+1}(kl) - \psi_i^m(kl)]/\Delta t$, with m being the time step number, and $\nabla^2 \psi_i(\mathbf{r},t)$ by

$$\nabla^2 \psi_i(kl) = \frac{1}{(\Delta r)^2}\left[\frac{2}{3}\sum_{\mathrm{NN}} + \frac{1}{6}\sum_{\mathrm{NNN}} - \frac{10}{3}\right]\psi_i(kl), \tag{5}$$

where NN and NNN mean the nearest neighbors and next-nearest neighbors, respectively, and the lattice point is $\mathbf{r}/\Delta r = (k,l)$. Here Δt is the time step and Δr is the lattice spacing. Both are dimensionless.

We have studied two systems in some detail. In both we choose $\epsilon = 0.1$ and use 1024×1024 lattice sites. In system 1, or the bigger system, we use $\Delta t = 0.02$ and $\Delta r = \pi/4$. In system 2, or the smaller system, we use $\Delta t = 0.01$ and $\Delta r = \pi/8$. In both we measured the vortices number and the system energy. We measured the vortex speed distribution only in the bigger system.

We prepare the system initially in a completely disordered state. The average magnitude $\overline{M}$ of the vector order parameter $\vec{\psi}$ at time t is calculated and the vortices' core regions are identified with those sites on which the order parameter magnitudes $|\vec{\psi}| < \overline{M}/4$. Usually each core has about ten sites

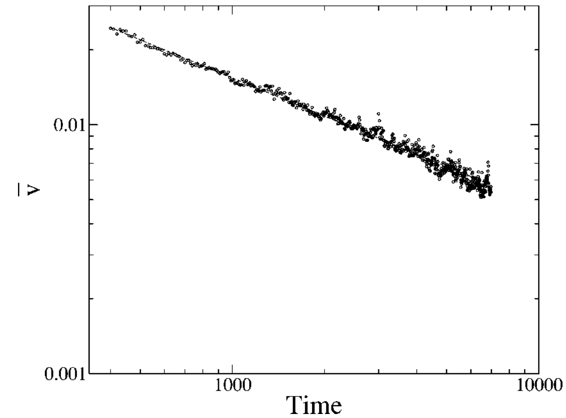

FIG. 2. The average speed $\overline{v(t)}$ of the vortices for the bigger system $(\Delta r = \pi/4)$. The speed of each vortex is calculated with $\Delta \tau = 5$. t^{-x} is used to fit the data. $x = 0.51 \pm 0.01$ for the system with $\Delta r = \pi/4$. The data are averaged over 60 different initial conditions.

in it. Here the coefficient 1/4 is appropriately chosen so that no vortices are missed and no irrelevant points are picked. A circular integration around each vortex produces 2π or -2π, which corresponds to two types of vortices of topological charges $+1$ and -1, respectively. In fact there are situations where we obtain charge 0. This is due to the nonzero area of the integration circle. When a pair of $+1$ and -1 vortices annihilate and the distance between them becomes smaller than the size of the integration circle, the circular integration will reflect the sum of the two charges, which is 0. However, the lifetime of these 0 charges are much smaller than the lifetime of the ± 1 vortices. So they do not affect our statistics. We find in our simulations that the numbers of positive and negative vortices are equal.

The position of a vortex is given by the center of its core region. Suppose the order parameter's magnitude at the core region is described by $M(x_i, y_i)$ with (x_i, y_i) belonging to the core region. Then by fitting $M(x_i, y_i)$ to the function $M(x,y) = A + B[(x-x_0)^2 + (y-y_0)^2]$ we can find the center (x_0, y_0).

The positions of each vortex at different times are recorded, and the speed is calculated using $v = \Delta d/\Delta \tau$. Here Δd is the distance that the vortex travels in time $\Delta \tau$. We have, simultaneously, recorded the number of vortices as a function of time and checked the scaling result given by Eq. (3).

III. NUMERICAL RESULTS

Every $\delta t = 10$ we compute the speed of each vortex with $\Delta \tau = 5$, i.e., $v = |\mathbf{r}(t+\Delta \tau) - \mathbf{r}(t)|/\Delta \tau$, with t increasing by step length δt and $\mathbf{r}$ being the position of the vortex. We found that the average speed of the vortices $\overline{v(t)}$ is proportional to t^{-x}, with $x = 0.51 \pm 0.01$ for the bigger system $(\Delta r = \pi/4)$ as shown in Fig. 2. Unlike the case for $L_v(t)$ extracted from n_v and $(E - E_0)$, we do not observe logarithmic correction for $\overline{v(t)}$. We cannot rule out such corrections appearing on a longer time scale, but they do not enter on the

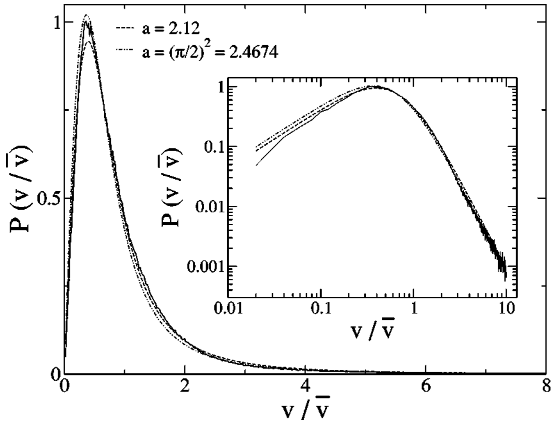

FIG. 3. The vortices' speed distribution probability density for the $\Delta r=\pi/4$ system $P(v/\overline{v}(t))$ (the solid line) fit to the function $P(x)=2ax/(1+ax^2)^2$, with $a=2.12$ and $x=v/\overline{v}(t)$. The theoretical curve with $a=(\pi/2)^2$ is also shown in the figure. The large speed tail of the distribution can be fit to t^{-y} with $y=3$. The inset shows the same data in the logarithmic scale, and it seems that the the theoretical curve fits the tail better. The data are averaged over 60 different initial conditions. In the calculation of the probability distribution we use the bin width of 0.02.

same time scale as for $L_v(t)$.

We compared the speed distribution at different times. They have approximately the same shape after being rescaled by the average speed. At early times this is clear. At late times there are fewer data points and the similarity between the two distributions at different times is not so apparent. Even at early times the number of data points are not enough to give a good fit to the distribution's long tail. So we rescale the speed data with the best fit to the average speed $\overline{v}(t) \propto t^{-0.51}$ and put the data for all times into one histogram as shown in Fig. 3. By this means we obtain better statistics. We find that the distribution can be well fit to the function

$$P(\tilde{v})=\frac{2a\tilde{v}}{(1+a\tilde{v}^2)^2}, \tag{6}$$

for a between 2 and 2.5. The best fit is for $a=2.12$. However, if we require that the average speed is given by the measured speed, then we must have $a=(\pi/2)^2=2.47$. The best fit and the most consistent fit are both shown in Fig. 3. The distribution has a long tail which is approximately $(v/\overline{v})^{-y}$ with $y=3$. If we just try to fit the long tail, then the best fit is given by $a=2.47$. These results are in excellent quantitative agreement with the theoretical prediction in Ref. [4].

In these results we have scaled the velocity with $\sim t^{-z}$ by taking $z=x$ just as the theory predicts. However, the value of scaling exponent z of the speed distribution is not very robust in our simulations. If we change the exponent z and use t^{-z} to rescale the speed distribution at different times, and they also have approximately the same shape. So the uncertainty of z is quite large. After being rescaled by t^{-z} and put into one histogram, the speed distribution for small and intermediate values of $\tilde{v}$ are somewhat dependent on the value of z.

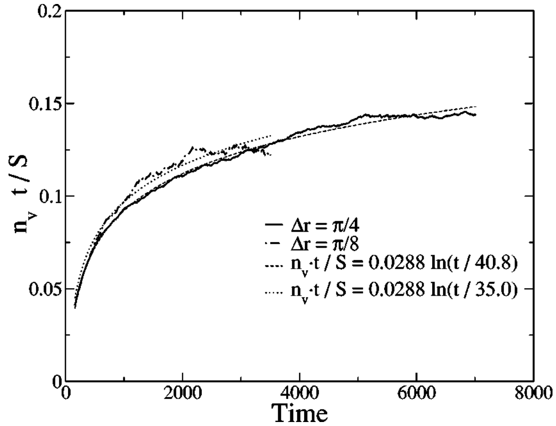

FIG. 4. The total number of the vortices per unit area, $n_v(t)/S$, times t, where $S=(1024\Delta r)^2$. In both systems $n_v t/S$ can be fit to $a\ \ln(t/t_0)$. The data from the large and the small systems are averaged over 68 and 58 different initial conditions, respectively.

However, the power-law tail is quite robust. We alter the value of z between 0.4 and 0.6, and find that the tail exponent changes by less than 0.1.

In both the larger and smaller systems, the vortex number densities have the same time dependence. We obtain $n_v \sim [t/\ln(t/t_0)]^{-1}$, where n_v is the number density of vortices (positive or negative) and t_0 is a constant. In Fig. 4, we show the data for $n_v t/S$. S is the area of the system. In Fig. 5, we show the data for the energy per unit area $(E-E_0)/S$ times t. We conclude that the energy density is proportional to the number density of the vortices.

IV. CONCLUSIONS

We have studied the growth kinetics of the nonconserved TDGL model in the case of $n=d=2$. We measured the speed probability distribution for the ± 1 vortices. At any given time with relatively few vortices, the statistics are poor. However, the accumulated data for all times when

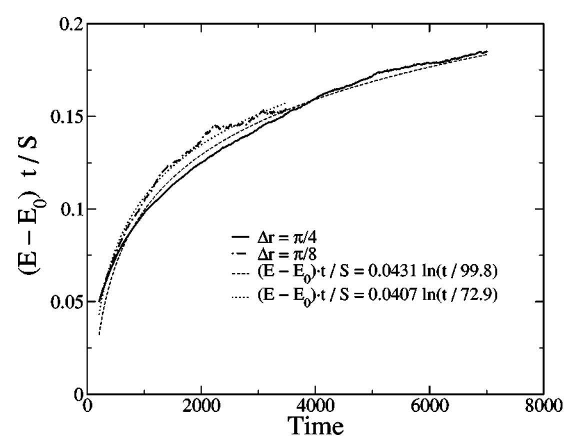

FIG. 5. The product of the system energy per unit area $(E-E_0)/S$ with t. The ground state energy is $E_0=-\epsilon^2 S/4$. The data can also be fit to $a\ \ln(t/t_0)$. The data from the large and the small systems are averaged over 68 and 58 different initial conditions, respectively.

scaled gives a scaling function with good statistics. Although the scaling exponent z is 0.5 with significant uncertainty, the large speed tail does takes the form of $(v/\overline{v})^{-y}$ with the exponent $y=3$. This is consistent with the theoretical prediction. The form of the distribution $P(\tilde{v})$ is quantitatively consistent with the theoretical prediction.

Why does the theory do so well? It was shown by Mazenko and Wickham [11] that one can construct a nontrivial self-consistent Gaussian theory for the order parameter if it is constrained to be evaluated near a vortex core. Such constraints occur naturally, for example, in averages over the vortex density. This suggests that the theory developed in Ref. [4] may be on a firmer footing than first thought.

According to the theory, the average speed should be proportional to the inverse of the correlation length $L(t)$. We did not observe any logarithmic correction in the average speed, although it appears in the correlation length when $n=d=2$. However, a logarithmic behavior may still exist. The time we used in our simulations may not be long enough to see the effect.

We also measured the number density of the vortices and the energy density of the two systems. Their time dependences both have a logarithmic correction, which is consistent with previous work.

ACKNOWLEDGMENT

This work was supported by the National Science Foundation under Contract No. DMR-0099324.

[1] A.J. Bray, Adv. Phys. **43**, 357 (1994).
[2] F. Liu and G.F. Mazenko, Phys. Rev. B **46**, 5963 (1992).
[3] M. Mondello and N. Goldenfeld, Phys. Rev. A **42**, 5865 (1990).
[4] G.F. Mazenko, Phys. Rev. Lett. **78**, 401 (1997).
[5] B. Yurke, A.N. Pargellis, T. Kovacs, and D.A. Huse, Phys. Rev. E **47**, 1525 (1993).
[6] A. Rutenberg and A.J. Bray, Phys. Rev. E **51**, 5499 (1995).
[7] A.N. Pargellis, P. Finn, J.W. Goodby, P. Panizza, B. Yurke, and P.E. Cladis, Phys. Rev. A **46**, 7765 (1992).
[8] F. Liu and G.F. Mazenko, Phys. Rev. B **45**, 6989 (1992).
[9] The case of systems with string defects, $n=d-1$, is discussed by G.F. Mazenko, Phys. Rev. E **59**, 1574 (1999).
[10] A.J. Bray, Phys. Rev. E **55**, 5297 (1999).
[11] G.F. Mazenko and R.A. Wickham, Phys. Rev. E **57**, 2539 (1998).